FEBS Letters 587 (2013) 2158–2163

FEBS Letters

journal homepage: www.FEBSLetters.org

Does bromodomain flexibility influence histone recognition?

Sandra Steiner, Andrea Magno, Danzhi Huang, Amedeo Caflisch *

Department of Biochemistry, University of Zurich, Winterthurerstrasse 190, CH-8057 Zurich, Switzerland

ARTICLE INFO

Article history:
Received 27 February 2013
Revised 10 May 2013
Accepted 13 May 2013
Available online 25 May 2013

Edited by Robert B. Russell

Keywords:
Molecular dynamics
Post-translational modification
Histone
Epigenetic target

ABSTRACT

Bromodomains are protein modules that selectively recognize histones by binding to acetylated lysines. Here, we have carried out multiple molecular dynamics simulations of 20 human bromodomains to investigate the flexibility of their binding site. Some bromodomains show alternative side chain orientations of three evolutionarily conserved residues: the Asn involved in acetyl-lysine binding and two conserved aromatic residues. Furthermore, for the BAZ2B and CREBBP bromodomains we observe occlusion of the binding site which is coupled to the displacement of the two aromatic residues. In contrast to available structures, the simulations reveal large variability of the binding site accessibility. The simulations suggest that the flexibility of the bromodomain binding site and presence of self-occluded metastable states influence the recognition of acetyl-lysine on histone tails.

1. Introduction

Bromodomains, protein modules of about 110 residues, recognize acetylated lysine side chains mainly in histones and are thus involved in transcriptional regulation [1,2]. In the human genome there are 46 proteins with a total of 61 different bromodomains, with up to six bromodomains per protein [3]. Due to the potential role of bromodomains in tumors and inflammation [4–6], large scale structural studies have been carried out with the ultimate goal to facilitate the discovery of small-molecule inhibitors able to interfere in the process of reading acetylated lysine [7]. Since 1999, when the first three-dimensional structure of a human bromodomain was solved [8], the crystal and/or solution structures of more than 40 human bromodomains have been reported [9,10]. All available structures show a conserved four-helix bundle topology (Fig. 1) in which the ZA-loop and BC-loop connect the first two α helices (called Z and A) and last two α helices (called B and C), respectively [10,11]. The acetyl-lysine binding site is very similar in all structures of bromodomains [10]. The BC-loop contributes the evolutionary conserved Asn side chain [12] which acts as hydrogen bond donor to the acetylated lysine side chain. Moreover, two conserved Tyr residues [13] are present in the ZA-loop and BC-loop, respectively (Fig. S1). In striking contrast to the abundance of available three-dimensional structures, there are only few computational studies on bromodomains [14–16]. In particular, it seems that the dynamic properties of human apo bromodomains have not been investigated yet by atomistic simulations. Here, we have studied the binding site flexibility of 20 bromodomains (covering seven of the eight families of human bromodomains) by explicit solvent MD simulations. The simulation results reveal a surprisingly high heterogeneity of the plasticity and accessibility of the acetyl-lysine binding site.

2. Results and discussion

A sequence alignment of the 20 simulated bromodomains with indication of important structural features and investigated key residues is given in Fig. S1. Family memberships are listed in Table S-I. The time series of root mean square deviation (RMSD) of the C_α atoms show that the overall fold of the simulated bromodomains is stable over the 1-μs time scale and 310 K temperature of the MD runs (Fig. S2). Most of the fluctuations are localized in the ZA-loop, BC-loop, and the termini (Fig. S3). The ZA-loop and BC-loop are involved in binding the histone tail whereas the termini are located far away from the acetyl-lysine binding site so that their motion can be neglected. Importantly, we observe multiple events of reversible rotation of the side chains investigated in the present study along the 0.5- to 1-μs time scale of the MD runs (Figs. S4 and S5). These rotations take place on a time scale about one order of magnitude smaller than the length of the simulations so that the following analysis is not marred by statistical errors.

We first investigated the flexibility of the conserved Asn which is directly involved in acetyl-lysine binding (i.e., Asn1944 in BAZ2B, Asn1168 in CREBBP, Asn1604 in TAF1(2), etc.). For most of the bromodomains studied here, there are many events of reversible

* Corresponding author. Fax: +41 (44) 635 68 62.
E-mail address: caflisch@bioc.uzh.ch (A. Caflisch).

0014-5793/$36.00
http://dx.doi.org/10.1016/j.febslet.2013.05.032

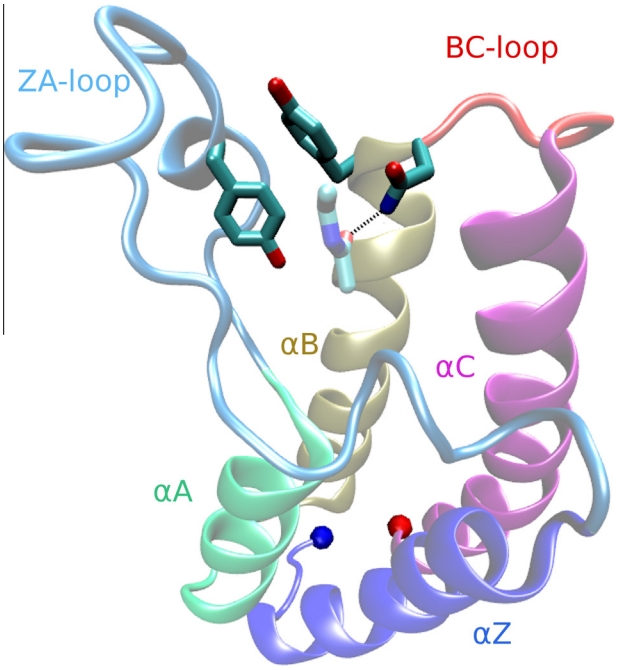

Fig. 1. Ribbon illustration of the crystal structure of the complex between CREBBP and acetyl-lysine (PDB code 3P1C). Each of the four α-helices and two binding site loops is displayed with a different color. The side chains of the conserved Tyr1125 of the ZA-loop, and Tyr1167-Asn1168 of the BC-loop are emphasized (sticks) together with the side chain of acetyl-lysine (sticks, light colors). The N-terminus and C-terminus are shown with a blue and red sphere, respectively.

rotations of the side chain amide of the conserved Asn (Figs. S4 and S5). The rotation (of about 180 degrees) around the χ_2 angle of the conserved Asn switches between an orientation in which the side chain $-NH_2$ group caps the C-terminal turn of α helix B (by donating a hydrogen bond to the backbone carbonyl of the n-4 upstream residue, e.g., the hydrogen bond between the Asn1168 side chain and the carbonyl group of residue 1164 in CREBBP) to a completely solvent exposed orientation of the $-NH_2$ group (Fig. 2, top). Note that the former orientation is observed in most (13 of 17) X-ray structures of the apo bromodomains used in this study (three of them have Thr (PHIP(2) and WDR9(2)) or Tyr (ASH1L) instead of the conserved Asn), as well as in the X-ray structures of BRD4(1) with three different diacetylated peptides (PDB codes 3UVW, 3UVY, and 3UW9) and in the CREBBP/acetyl-lysine complex (PDB code 3P1C). Interestingly, in seven of the 17 bromodomains the Asn $-NH_2$ group is oriented towards the solvent during more than one third of the simulation time (Figs. S4 and S5). These bromodomains are: TAF1L(2) (90% of the snapshots with solvent-exposed orientation of the Asn $-NH_2$ group), TAF1(2) (81%), TAF1(1) (68%), GCN5L2 (44%), ATAD2 (43%), BAZ2B (39%), and PB1(2) (38%). For TAF1L(2), TAF1(2), and TAF1(1) (all belonging to a single clade of family VII in the bromodomain phylogenetic tree [10]) the solvent exposed orientation of the Asn -NH_2 group is stabilized by a water-bridged hydrogen bond between the Asn side chain carbonyl and the hydroxyl group of the Ser in position n-4 upstream (Fig. 2, bottom). It has to be noted that most bromodomains have Ala or Cys at position n-4 upstream of the conserved Asn so that these side chains cannot form a (water-bridged) hydrogen bond. Note also that an in-depth analysis of the water molecules in the

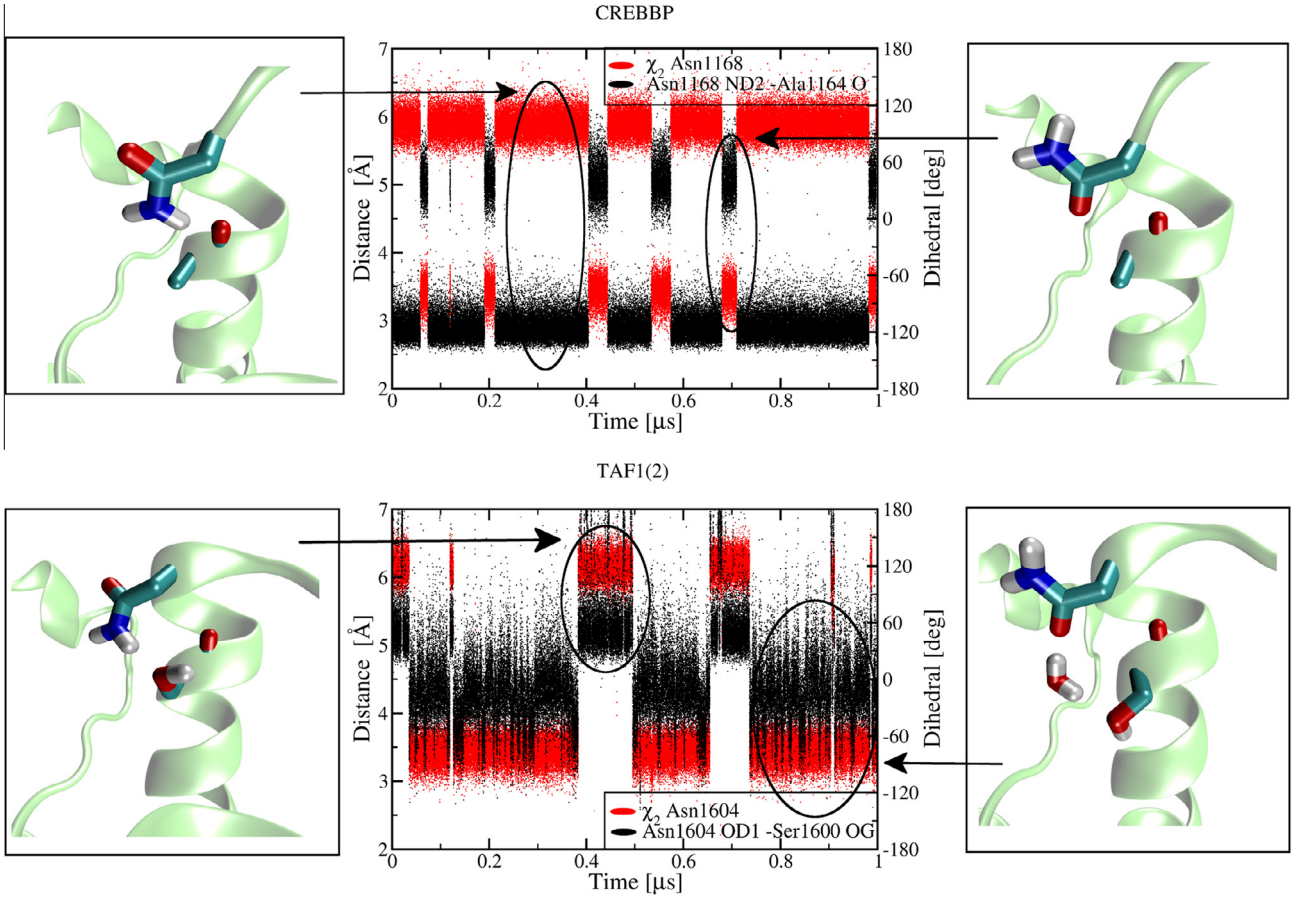

Fig. 2. Rotational flexibility of the conserved Asn side chain as observed in MD simulations of CREBBP (top) and TAF1(2) (bottom). (Middle) Time series of Asn χ_2 angle of conserved Asn (red) and distance between Asn side chain and residue n-4 upstream (black). (Left and right) Representative MD snapshots.

binding site along the MD trajectories goes beyond the scope of this paper and will be presented elsewhere together with a comparison with the five water molecules that seem to be conserved in the crystal structures [10].

We further analyzed the motion of residues adjacent to the conserved Asn to shed light onto the accessibility of the acetyl-lysine binding site. The MD trajectories of some of the 20 simulated bromodomains unmask a large flexibility of the side chain of the evolutionary conserved Tyr (Phe in BAZ2B and SMARCA4) in the BC-loop, i.e., the residue preceding in the sequence the Asn involved in acetyl-lysine binding (Figs. S4 and S5). The side chain of this Tyr (or Phe) rotates from an inward orientation in which the aromatic ring is part of the binding site surface (χ_1 angle in trans) to an outward orientation in which the same side chain points towards the exterior surface of the bromodomain (χ_1 angle values around −60 degrees) (Fig. 3). The five bromodomains with a population larger than 10% of the outward orientation of the BC-loop Tyr (or Phe) side chain are BRDT(1) (100%), CREBBP (31%), BAZ2B (24%), SMARCA4 (21%), and BRD1 (11%). This simulation result is a novel finding because only two of the more than 50 bromodomain crystal and solution structures (i.e., the X-ray structure of BRDT(1) and the NMR structure of KIAA1240, PDB codes 2RFJ and 2DKW, respectively) show a similar outward orientation of the side chain of the conserved Tyr on the BC-loop. Note that in contrast to the solution structure, the crystal structure of KIAA1240 (PDB code 3LXJ) does not show the outward orientation of the conserved Tyr.

To further investigate the influence of the displacement of the BC-loop Tyr on the binding site accessibility, two-dimensional histograms were calculated for each of the 20 simulated bromodomains (Figs. 3(b) and S6). According to the two-dimensional histograms the 20 bromodomains can be assigned to three different groups. The largest group consists of the bromodomains with an open binding site, and in which the side chain of the conserved Tyr of the BC-loop is part of the binding site surface (χ_1 angle always in the trans orientation, e.g., TAF1(2)). The second group includes the bromodomains in which the conserved Tyr changes its orientation without affecting the binding site accessibility (e.g., BRD1 and SMARCA4). The third group includes the bromodomains

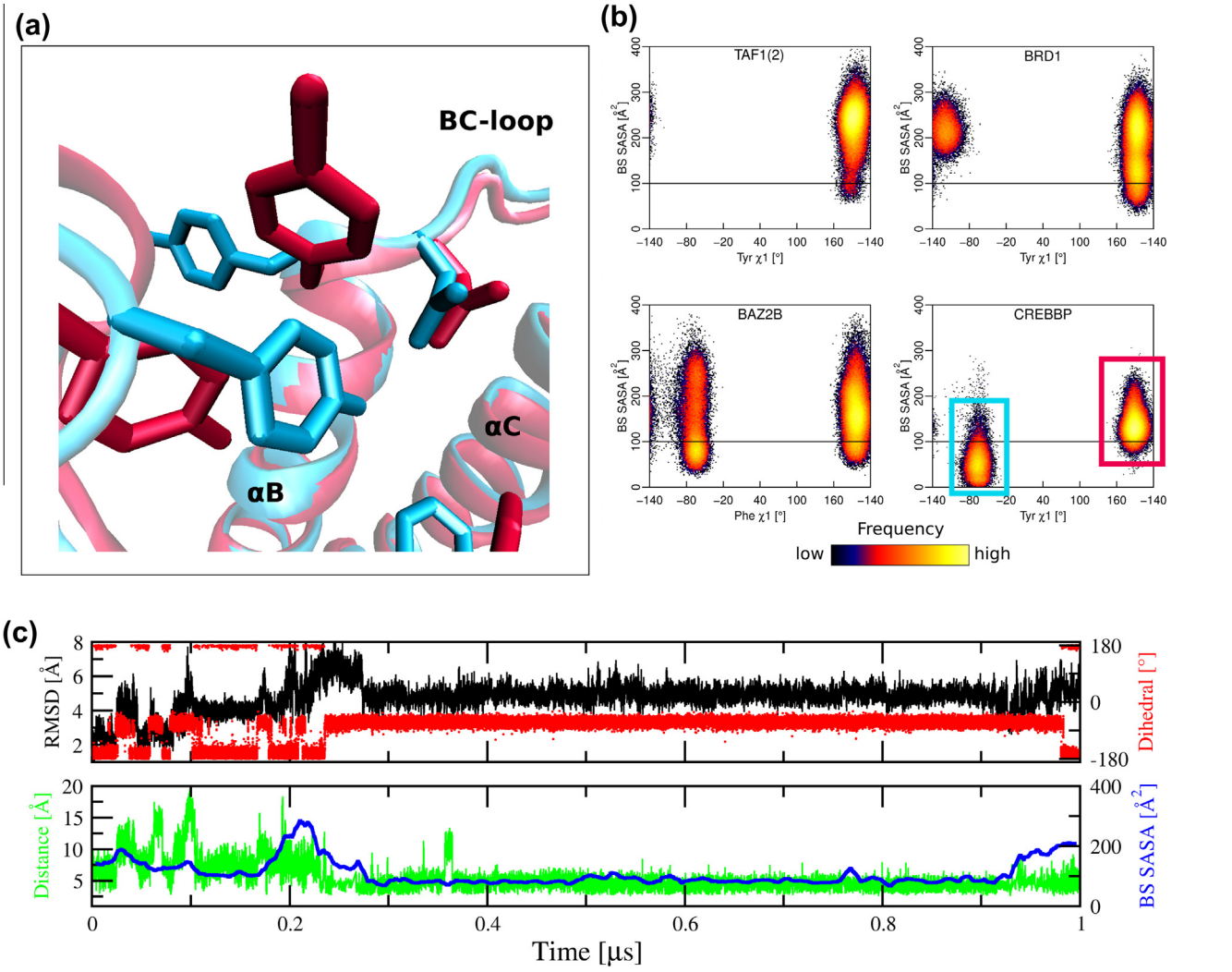

Fig. 3. Swapping out of the aromatic residue preceding the conserved Asn in the BC-loop. (a) Representative snapshots extracted from the MD simulations of CREBBP. (b) Two-dimensional histograms of binding site solvent accessible surface area (SASA) versus side chain χ_1 angle of the conserved Tyr (Phe in BAZ2B) in the BC-loop. The horizontal line at 100 Å^2 is an arbitrary threshold drown solely to help the eye. The cyan and red rectangles in the histogram of CREBBP emphasize the metastable states corresponding to the cyan and red structures, respectively, in panel (a). The black to yellow coloring of frequency values follows a logarithmic scale and is shown in the legend bar. (c) Time series of four geometrical variables used to analyze the binding site. This panel shows run 2 of BAZ2B while the equivalent time series for the other MD runs are shown in Figs. S7–S10. The variables are the RMSD of the C_α atoms of the ZA-loop from the crystal structure (black), the Phe1943 χ_1 dihedral angle (red), the binding site SASA (blue, running average calculated over time intervals of 10 ns for clarity), and the distance between the hydroxyl oxygen of Tyr1901 and the nitrogen atom of the Asn1944 side chain (green).

in which the outward orientation of the BC-loop Tyr promotes a rearrangement of other binding site residues resulting in a partially occluded, i.e., shallower binding site (e.g., BAZ2B and CREBBP, Figs. 3(b) and 4). More precisely, one observes large fluctuations of the ZA-loop that are associated frequently with the swapping out of the BC-loop Tyr (Figs. 3(c), S7 and S8) and with changes in the accessibility of the binding site (Figs. S9 and S10). In particular, in the BAZ2B and CREBBP simulation segments during which the conserved Tyr of the BC-loop points outward, the conformational plasticity of the ZA-loop results (in 20% to 25% of the saved snapshots) in the formation of a direct hydrogen bond between Asn1168 and ZA-loop Tyr1125 in CREBBP (Figs. 3(c) and 4), and Asn1944 and ZA-loop Tyr1901 in BAZ2B. Note that these two side chains are separated by two water molecules in the X-ray structures (PDB codes 3DWY and 3G0L). In essence, it emerges from the MD trajectories that the ZA-loop Tyr side chain can occupy the same position and can be stabilized by the same hydrogen bond to Asn as the natural ligand acetyl-lysine (Fig. 4).

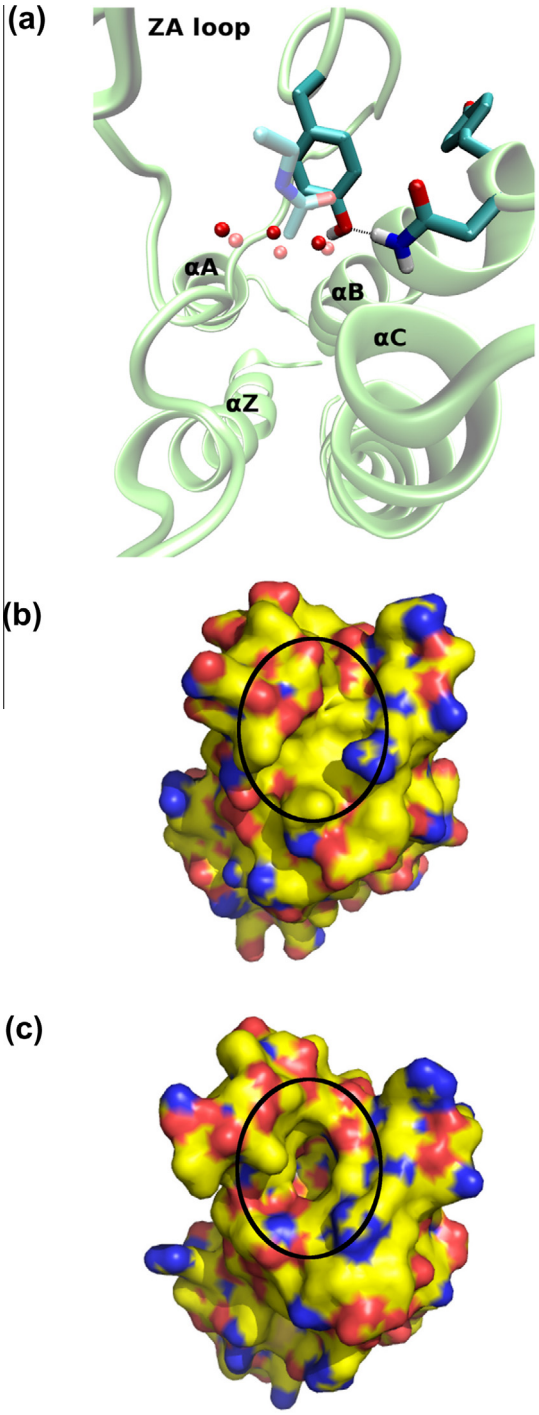

Fig. 4. Occlusion of the acetyl-lysine binding site by the conserved Tyr of the ZA-loop. (a) The ribbon structure is a representative MD snapshot of the CREBBP simulations in which the conserved Tyr of the ZA-loop is involved in a hydrogen bond with the Asn that binds acetyl-lysine. The three conserved side chains (sticks) are shown together with three water molecules (red spheres). The position of acetyl-lysine (light-colored sticks) and three water molecules (light red spheres) from the crystal structure of the CREBBP/acetyl-lysine complex (PDB code 3P1C) was obtained by structural superposition of the C_α atoms. Surface representation of a representative MD snapshot with partially occluded, i.e., shallower, binding site (b) and the crystal structure of CREBBP (PDB code 3P1C) (c). The color coding reflects atomic elements (carbon, nitrogen, and oxygen atoms in yellow, blue, and red, respectively). The location of the acetyl-lysine binding site is indicated with a black oval.

The ZA-loop shows significant plasticity and large deviations from the crystal structure (Figs. 3(c), S7 and S8). This flexibility is consistent with the structural heterogeneity of the ZA-loop observed by overlapping the available X-ray structures [10] as well as with the length of the ZA-loop (about 25–30 residues, Fig. S1). Figs. 3(c), S9 and S10 show that the displacement of the ZA-loop influences the binding site accessibility (note that 4 of the 6 residues used to calculate the binding site accessibility are in the ZA-loop). In particular, the accessibility can change significantly in the MD trajectory segments during which the ZA-loop RMSD from the crystal structure is large, while the accessibility is less variable in segments with mainly rigid ZA-loop. Interestingly, the ZA-loop conformational flexibility has been shown to play an important role at the protein-protein interface for HIV-1 Tat binding to bromodomain PCAF [14]. In the present simulations of CREBBP and BAZ2B, the rearrangement of the ZA-loop and thus of several residues lining the binding site reduces its aperture which could hinder histone peptide recognition.

In conclusion, the MD trajectories reveal a heterogeneous flexibility of the acetyl-lysine binding site in different bromodomains. The analysis of the trajectories shows that the accessibility of the binding site ranges from fully preserved (for the majority of bromodomains) to almost completely inaccessible during simulation segments of hundreds of ns (e.g., in BAZ2B and CREBBP). Of practical importance, the presence of metastable states in a small subset of bromodomains can be exploited [17–19] to design selective small-molecule inhibitors few of which have been reported as of today [4,20–23]. The present simulation results shed some light on the binding mechanism of histone tails to bromodomains which seems to be mainly conformational selection, though a (partial) induced fit cannot be definitively excluded. More precisely, with the present simulations of apo bromodomains it is not possible to exclude a ligand-promoted displacement of some of the side chains in the acetyl-lysine binding site. The self-occluded conformation of the acetyl-lysine binding groove suggests a possible auto-regulatory mechanism of histone tail recognition and binding.

3. Methods

The coordinates of the 20 bromodomains were downloaded from the protein database [24]. To reproduce neutral pH conditions the side chains of aspartates and glutamates were negatively charged, those of lysines and arginines were positively charged, and the histidine side chains were neutral. For each bromodomain the crystal water molecules close to the binding site and with low B factor value were kept while the remaining water molecules were deleted. For most bromodomains a B-factor of 15 $Å^2$ was used as threshold for keeping crystallographic water molecules. For the few bromodomains with overall higher B-factors a threshold of 30 $Å^2$ was used. With this arbitrary choice of thresholds between

4 and 15 crystal water molecules were retained for each bromodomain. Importantly, in our simulations the structured water molecules exchange rapidly (residence times ranging from 0.01 to 1 ns) with the water molecules in the bulk solvent. Furthermore, in test simulations without crystal water molecules, bulk water molecules rapidly occupied the conserved positions in the binding site. Thus, the exact number of kept crystal waters does not influence the results of our simulations because individual runs have a length of 0.5 or 1 μs.

Subsequently, the structure was solvated in a water box whose size was chosen to have a minimal distance of 11 Å between the boundary and any atom of the protein. Solvation water molecules within 2.4 Å of any heavy atom of the protein or crystal water were removed. The simulation system contained sodium and chloride ions to approximate an ionic strength of about 150 mM and to compensate for the total charge of each bromodomain. The MD simulations were carried out with Gromacs 4.5.4 [25] using the CHARMM PARAM22 force field [26] and the TIP3P model of water [27].

Periodic boundary conditions were applied and electrostatic interactions were evaluated using the particle-mesh Ewald summation method [28]. The van der Waals interactions were truncated at a cutoff of 10 Å. The temperature of 310 K was kept constant by an external bath with velocity rescaling [29] and the pressure was kept close to 1 atm by the Berendsen barostat. The SHAKE algorithm was used to fix the covalent bonds involving hydrogen atoms. The integration time step was 2 fs and snapshots were saved every 10 ps and 4 ps for the 1-μs and 0.5-μs runs, respectively.

Multiple independent MD runs of 1 μs each were carried out for four bromodomains belonging to four different families: BAZ2B (family V), BRD1 (IV), CREBBP (III), and TAF1(2) (VII). In addition, 16 bromodomains covering all but one of the families were simulated for 0.5 μs each (Table S-I). The crystal structures solved by the Structural Genomics Consortium [10] were used as starting conformations.

The solvent accessible surface area (SASA) was calculated with the SURF tool of Wordom, using the GEPOL algorithm [30,31] and 1.4 Å as radius of the water probe. The following procedure was used to define the acetyl-lysine binding site for the SASA calculation. First, using the X-ray structure of the CREBBP/acetyl-lysine complex (PDB code 3P1C) residues were selected which had at least three heavy atoms within 6 Å of the ligand. From this set Tyr1167 and Asn1168 were excluded to avoid redundancy in the two variables used for the two-dimensional histograms. Of the six remaining residues (Pro1110, Phe1111, Val1115, Tyr1125, Ala1164, Val1174), only the side chain atoms were used to evaluate the binding site SASA. For the other bromodomains the equivalent residues upon structural overlap were chosen. Robustness of the selection of binding site residues is shown in Fig. S11.

Acknowledgments

The simulations were carried out on the Schrödinger cluster at the University of Zurich. This work was supported by a grant of the Swiss National Science Foundation to A.C.

Appendix A. Supplementary data

Supplementary data associated with this article can be found, in the online version, at http://dx.doi.org/10.1016/j.ejor.2012.04.007.

References

[1] Zeng, L. and Zhou, M.-M. (2002) Bromodomain: an acetyl-lysine binding domain. FEBS Lett. 513 (1), 124–128.
[2] Filippakopoulos, P. and Knapp, S. (2012) The bromodomain interaction module. FEBS Lett. 586 (17), 2692–2704.
[3] Arrowsmith, C.H., Bountra, C., Fish, P.V., Lee, K. and Schapira, M. (2012) Epigenetic protein families: a new frontier for drug discovery. Nat. Rev. Drug Discov. 11 (5), 384–400.
[4] Filippakopoulos, P., Qi, J., Picaud, S., Shen, Y., Smith, W.B., Fedorov, O., Morse, E.M., Keates, T., Hickman, T.T., Felletar, I., Philpott, M., Munro, S., McKeown, M.R., Wang, Y., Christie, A.L., West, N., Cameron, M.J., Schwartz, B., Heightman, T.D., Thangue, N.L., French, C.A., Wiest, O., Kung, A.L., Knapp, S. and Bradner, J.E. (December 2010) Selective inhibition of bet bromodomains. Nature 468 (7327), 1067–1073.
[5] Zuber, J., Shi, J., Wang, E., Rappaport, A.R., Herrmann, H., Sison, E.A., Magoon, D., Qi, J., Blatt, K., Wunderlich, M., Taylor, M.J., Johns, C., Chicas, A., Mulloy, J.C., Kogan, S.C., Brown, P., Valent, P., Bradner, J.E., Lowe, S.W. and Vakoc, C.R. (2011) Rnai screen identifies Brd4 as a therapeutic target in acute myeloid leukaemia. Nature 478 (7370), 524–528.
[6] Dawson, M.A., Kouzarides, T. and Huntly, B.J. (2012) Targeting epigenetic readers in cancer. N. Engl. J. Med. 367 (7), 647–657. PMID: 22894577.
[7] Hewings, D.S., Rooney, T.P.C., Jennings, L.E., Hay, D.A., Schofield, C.J., Brennan, P.E., Knapp, S. and Conway, S.J. (2012) Progress in the development and application of small molecule inhibitors of bromodomain-acetyl-lysine interactions. J. Med. Chem. 55 (22), 9393–9413.
[8] Dhalluin, C., Carlson, J.E., Zeng, L., He, C., Aggarwal, A.K. and Zhou, M.-M. (1999) Structure and ligand of a histone acetyltransferase bromodomain. Nature 399 (6735), 491–496.
[9] Mujtaba, S., Zeng, L. and Zhou, M. (2007) Structure and acetyl-lysine recognition of the bromodomain. Oncogene 26 (37), 5521–5527.
[10] Filippakopoulos, P., Picaud, S., Mangos, M., Keates, T., Lambert, J.-P., Barsyte-Lovejoy, D., Felletar, I., Volkmer, R., Müller, S., Pawson, T., Gingras, A.-C., Arrowsmith, C.H. and Knapp, S. (2012) Histone recognition and large-scale structural analysis of the human bromodomain family. Cell 149 (1), 214–231.
[11] Vidler, L.R., Brown, N., Knapp, S. and Hoelder, S. (2012) Druggability analysis and structural classification of bromodomain acetyl-lysine binding sites. J. Med. Chem. 55 (17), 7346–7359.
[12] Owen, D.J., Ornaghi, P., Yang, J.-C., Lowe, N., Evans, P.R., Ballario, P., Neuhaus, D., Filetici, P. and Travers, A.A. (2000) The structural basis for the recognition of acetylated histone H4 by the bromodomain of histone acetyltransferase Gcn5p. EMBO J. 19 (22), 6141–6149.
[13] Furdas, S.D., Carlino, L., Sippl, W. and Jung, M. (2012) Inhibition of bromodomain-mediated protein–protein interactions as a novel therapeutic strategy. Med. Chem. Commun. 3, 123–134.
[14] Pantano, S., Marcello, A., Ferrari, A., Gaudiosi, D., Sabò, A., Pellegrini, V., Beltram, F., Giacca, M. and Carloni, P. (2006) Insights on HIV-1 Tat:P/CAF bromodomain molecular recognition from in vivo experiments and molecular dynamics simulations. Proteins: Struct. Funct. Bioinform. 62 (4), 1062–1073.
[15] Pizzitutti, F., Giansanti, A., Ballario, P., Ornaghi, P., Torreri, P., Ciccotti, G. and Filetici, P. (2006) The role of loop ZA and Pro371 in the function of yeast Gcn5p bromodomain revealed through molecular dynamics and experiment. J. Mol. Recognit. 19 (1), :1–9.
[16] Eichenbaum, K.D., Rodríguez, Y., Mezei, M. and Osman, R. (2010) The energetics of the acetylation switch in p53-mediated transcriptional activation. Proteins: Struct. Funct. Bioinform. 78 (2), 447–456.
[17] Ekonomiuk, D., Su, X.-C., Ozawa, K., Bodenreider, C., Lim, S.P., Otting, G., Huang, D. and Caflisch, A. (August 2009) Flaviviral protease inhibitors identified by fragment-based library docking into a structure generated by molecular dynamics. J. Med. Chem. 52 (15), 4860–4868.
[18] Zhao, H., Huang, D. and Caflisch, A. (September 2012) Discovery of tyrosine kinase inhibitors by docking into an inactive kinase conformation generated by molecular dynamics. ChemMedChem 7, 1983–1990.
[19] Laine, E., Martnez, L., Ladant, D., Malliavin, T. and Blondel, A. (August 2012) Molecular motions as a drug target: mechanistic simulations of anthrax toxin edema factor function led to the discovery of novel allosteric inhibitors. Toxins (Basel) 4 (8), 580–604.
[20] Nicodeme, E., Jeffrey, K.L., Schaefer, U., Beinke, S., Dewell, S., Chung, C.-W., Chandwani, R., Marazzi, I., Wilson, P., Coste, H., White, J., Kirilovsky, J., Rice, C.M., Lora, J.M., Prinjha, R.K., Lee, K. and Tarakhovsky, A. (December 2010) Suppression of inflammation by a synthetic histone mimic. Nature 468 (7327), 1119–1123.
[21] Gerona-Navarro, G., Yoel-Rodrguez, Mujtaba, S., Frasca, A., Patel, J., Zeng, L., Plotnikov, A.N., Osman, R. and Zhou, M.-M. (February 2011) Rational design of cyclic peptide modulators of the transcriptional coactivator CBP: a new class of p53 inhibitors. J. Am. Chem. Soc. 133 (7), :2040–2043.
[22] Chung, C.-W., Dean, A.W., Woolven, J.M. and Bamborough, P. (January 2012) Fragment-based discovery of bromodomain inhibitors part 1: Inhibitor binding modes and implications for lead discovery. J. Med. Chem. 55 (2), 576–586.
[23] Bamborough, P., Diallo, H., Goodacre, J.D., Gordon, L., Lewis, A., Seal, J.T., Wilson, D.M., Woodrow, M.D. and Chung, C.-W. (January 2012) Fragment-based discovery of bromodomain inhibitors part 2: Optimization of phenylisoxazole sulfonamides. J. Med. Chem. 55 (2), 587–596.
[24] Bernstein, F.C., Koetzle, T.F., Williams, G.J., Meyer Jr., E.F., Brice, M.D., Rodgers, J.R., Kennard, O., Shimanouchi, T. and Tasumi, M. (1978) The protein data

bank: a computer-based archival file for macromolecular structures. Arch. Biochem. Biophys. 185 (2), 584–591.
[25] Spoel, D.V.D., Lindahl, E., Hess, B., Groenhof, G., Mark, A.E. and Berendsen, H.J.C. (December 2005) Gromacs: fast, flexible, and free. J. Comput. Chem. 26 (16), 1701–1718.
[26] MacKerell, A.D., Bashford, D., Bellott, M., Dunbrack, R.L.J., et al. (1998) All-atom empirical potential for molecular modeling and dynamics studies of proteins. J. Phys. Chem. B 102, 35863616.
[27] Jorgensen, W.L., Chandrasekhar, J., Madura, J., Impey, R.W. and Klein, M.L. (1983) Comparison of simple potential functions for simulating liquid water. J. Chem. Phys. 79, 926935.
[28] Darden, T., York, D. and Pedersen, L.G. (1993) Particle mesh Ewald: an nlog(n) method for Ewald sums in large systems. J. Chem. Phys. 98, 10089.
[29] Bussi, G., Donadio, D. and Parrinello, M. (2007) Canonical sampling through velocity rescaling. J. Chem. Phys. 126 (1), 014101.
[30] Seeber, M., Cecchini, M., Rao, F., Settanni, G. and Caflisch, A. (October 2007) Wordom: a program for efficient analysis of molecular dynamics simulations. Bioinformatics 23 (19), 2625–2627.
[31] Seeber, M., Felline, A., Raimondi, F., Muff, S., Friedman, R., Rao, F., Caflisch, A. and Fanelli, F. (April 2011) Wordom: a user-friendly program for the analysis of molecular structures, trajectories, and free energy surfaces. J. Comput. Chem. 32 (6), 1183–1194.